Tunneling and decay dynamics of H1Sg+ outer well states in hydrogen

Reinhold, E.M.

published in
Journal of Chemical Physics
2000

DOI (link to publisher)
10.1063/1.481719

document version
Publisher's PDF, also known as Version of record

Tunneling and decay dynamics of $\bar{H}^1\Sigma_g^+$ outer well states in hydrogen

E. Reinhold,[a] W. Hogervorst, and W. Ubachs
Department of Physics and Astronomy, Vrije Universiteit, De Boelelaan 1081, 1081 HV Amsterdam, The Netherlands

(Received 29 February 2000; accepted 29 March 2000)

We present an experimental study of the decay dynamics of rovibrational states confined in the outer minimum of the $H\bar{H}\,^1\Sigma_g^+$ potential of the hydrogen molecule. Specific (v,J) quantum states are populated using a two-step excitation process involving a pulsed extreme ultraviolet laser source. Decay products are selectively probed with additional laser pulses, using the timing of these pulses to determine lifetimes. The competition between dissociation and ionization, occurring at short internuclear distance after tunneling through the potential barrier, is addressed. Observed lifetimes and decay channels of $\bar{H}$ levels are consistent with a semiclassical description of tunneling of the nuclear motion through the potential barrier towards small internuclear distance. For the HD isotopomer breaking of the $g-u$ symmetry is found to strongly affect the decay dynamics. © *2000 American Institute of Physics.* [S0021-9606(00)00624-3]

I. INTRODUCTION

Molecular hydrogen, the smallest neutral molecule, is a benchmark system for the study of competing decay processes of excited states, experimentally as well as theoretically. Of the large number of studies we mention only a few. Chupka and Berkowitz observed, already 30 years ago, competitive decay by pre-ionization and predissociation.[1] Since then many studies have been performed exciting H_2 from its electronic ground state with short wavelength photons up to 50 eV, produced in synchrotrons. Dissociative decay was investigated by monitoring Lyman and Balmer emission from the atomic H-fragments in excited states,[2,3] even in coincidence when two excited H-atoms were produced.[4] Decay by autoionization was detected with angular and kinetic-energy resolution.[5] In these studies super-excited states of u symmetry were probed, however, limited to the Franck–Condon region, i.e., states which have vibrational wave functions that overlap with the $X\,^1\Sigma_g^+$, $v=0$ ground state, located in a narrow region of internuclear distance.

Lasers and multiphoton excitation have extended the scope of these studies on competing decay phenomena. Singlet g Rydberg states were investigated using 1 XUV (extreme ultraviolet) + 1 UV (ultraviolet) double resonance excitation with the $B\,^1\Sigma_u^+$ state as intermediate.[6] A similar laser scheme was employed to probe the $H^+ + H^-$ ion-pair production channel.[7] Via two-photon excitation of the $EF\,^1\Sigma_g^+$ intermediate state, again the u states were probed,[8] accessing states in a much wider range of internuclear distances than in earlier studies due to the extended vibrational wave function of the EF state. At the $(n=3)$ dissociation limit the closing of the parent ionization channel was observed, accompanied by the opening of the dissociation channel. This phenomenon was probed by $(3+1)$ REMPI (resonantly enhanced multiphoton ionization)[9] and by (XUV+visible) two-frequency photoionization.[10]

The theoretical framework of multichannel-quantum-defect theory (MQDT), developed to explain features of coupling to continuum states, was refined by Jungen *et al.* to accurately reproduce the observations on states of u symmetry[11] and of g symmetry.[12]

The present experimental study focuses on the decay dynamics of resonances of the hydrogen molecule, confined to large internuclear separation, at energies above the $(n=2)$ dissociation limit. In the outer well of the $H\bar{H}\,^1\Sigma_g^+$ double-well potential, denoted $\bar{H}$, a series of narrow, long-lived rovibrational levels exist, part of which lie above the ionization threshold. Accounts on the spectroscopy of these levels were published before[13] in combination with *ab initio* calculations that were shown to agree within 1 cm^{-1}.[14] In the HD isotope the study was extended to the $\bar{B}$ state (short for the outer-well part of the $B''\bar{B}\,^1\Sigma_u^+$ potential), which has a potential shape similar to the $\bar{H}\,^1\Sigma_g^+$ state. A spectroscopic study has revealed[15] that nonadiabatic coupling of these two states, due to a complete breakdown of the $g-u$ symmetry has to be taken into account.

Here we focus on the decay dynamics of individual $\bar{H}\,^1\Sigma_g^+$ (v,J) quantum states. Tunneling through the potential barrier, described within a semiclassical model, inhibits autoionization and predissociation due to interaction with states at small internuclear distance R. It is shown that the symmetry breaking considerably influences the lifetimes of the observed states in the case of HD.

II. EXPERIMENT

The experimental technique to excite singlet gerade resonances in the hydrogen molecule has been described earlier;[13–16] here some modifications, made to identify decay products and to determine lifetimes, will be discussed in detail. States of the singlet gerade manifold are populated using

[a]Electronic mail: elmar@nat.vu.nl

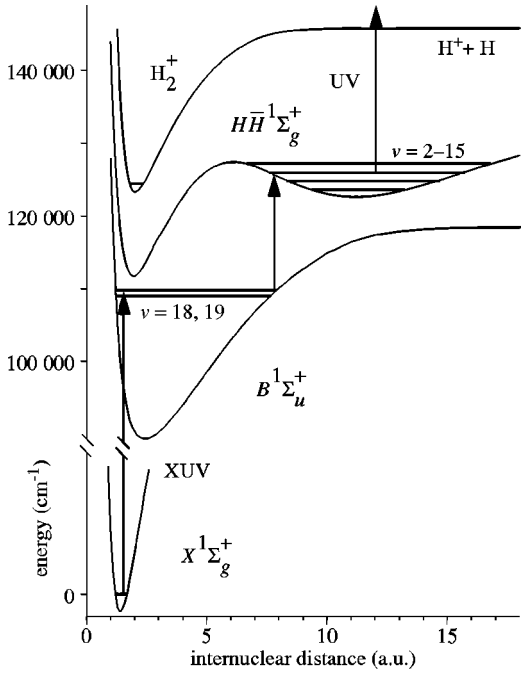

FIG. 1. Scheme for resonance-enhanced two-step excitation of the $\bar{H}$ state via intermediate B vibrational levels. Population is probed by dissociative ionization with a delayed laser pulse, producing H^+ ions.

a resonance-enhanced two-step laser excitation scheme: a narrowband, extreme ultraviolet (XUV) pulse (3–5 ns), produced in a third harmonic process in a pulsed gas jet, selectively excites a single rovibrational $B\,^1\Sigma_u^+$ quantum state. The intense UV radiation that originates from the XUV generation process is filtered out of the XUV-beam before reaching the interaction region with a noncollinear phase-matching setup described in Ref. 16. Subsequently a pulsed dye laser in the visible or near-infrared range excites the states to be investigated; in view of the short lifetime of the intermediate states (typically 1 ns) both laser pulses are temporally overlapped in the interaction zone. The decay dynamics of the excited gerade states is investigated through detection of ions, which are either decay products themselves or created by absorption of an additional photon; for this purpose a third laser pulse is applied in part of the experiments, using different wavelengths and timings to obtain more detailed information on the decay process. Ions are extracted by a pulsed electric field, delayed by $\approx$500 ns with respect to the laser pulses and detected by an electron multiplier. H_2^+ and H^+ ions are separated by their time-of-flight in a drift tube. (Accordingly D_2^+, HD^+, and D^+ in the cases of D_2 and HD; this will be implicitly assumed below.)

After exciting $\bar{H}$ states by the two excitation pulses, the third pulse is delayed to selectively probe long-lived excited states by dissociative ionization, i.e., ionization reaching the dissociative continuum of H_2^+ as displayed in Fig. 1

$$H_2^{**} \rightarrow H + H^+ + e^-. \tag{1}$$

The second laser is tuned and H^+ signal is registered as a function of wavelength, together with the H_2^+ signal.

In order to study various aspects of the dynamics of the $\bar{H}$ state and to identify different decay processes, laser pulses of different wavelengths are used for ionization: Either a 355 nm pulse from the third harmonic of a Nd:YAG laser is used, or another Nd:YAG-pumped dye laser with a tuning range of 420–440 nm is employed. The latter provides sufficient photon energy for dissociative ionization of H_2 molecules in the $\bar{H}$ state and to cover the Balmer-γ (B_γ) line H($n=2$)$\rightarrow$($n=5$).

The timing of the ionization pulse with respect to the other pulses is controlled on-line by an external trigger of the Q-switches of the Nd:YAG lasers (Stanford Research SRS-DGD535). For lifetime measurements in the time domain the H^+ signal is recorded as a function of the delay of the last laser pulse. An exponential with a variable offset is fitted to the signal; in each measurement the delay range covers at least four times the decay time to allow for a reliable fit. The fit is started at a delay of 10 ns to avoid artefacts caused by temporal overlap of the ionization pulse with the excitation pulses. Hence a time domain measurement is only possible for lifetimes $\tau > 5$ ns and accuracy is significantly reduced for $\tau < 10$ ns.

A sufficient signal-to-noise ratio is obtained by averaging over several pulses with the same delay and by varying the delay time in small steps. This results in total measurement times of up to seven minutes for a decay curve at a repetition rate of 10 Hz. Longer averaging times do not improve the measurements because the dye lasers producing the XUV radiation and the second pulse in the visible, both fixed on the resonance frequencies without stabilization, tend to drift in wavelength. Residual effects of the wavelength drift are minimized by repetitively varying the delay in both time directions.

III. RESULTS AND DISCUSSION

Observable effects of the decay dynamics are shortening of lifetimes and the formation of different decay products. Variations of lifetimes are either observed indirectly through line broadening or directly in a time domain measurement; decay products and corresponding decay channels are identified by the formation of ions, including fragment ions, under different excitation conditions.

A. Broadened lines and lifetimes

Considerable line broadening is observed for the highest vibrational levels below the barrier in the $H\bar{H}$ potential in all isotopomers H_2, D_2, and HD. Above the barrier energy no $H\bar{H}$ levels can be identified. Figure 2 shows a sequence of $\bar{H}$ levels in D_2 converging to the barrier energy; linewidths increase from laser linewidth in $v=20$ to 3 cm^{-1} in $v=22$, obscuring the rotational structure. At the energy where the $v=23$ level is predicted, which should lie very close to the $H\bar{H}$ potential barrier, a strong resonance is observed that shows an irregular lineshape; actually most of the broadened lines deviate clearly from a Lorentzian. In addition to line broadening strong variations in the D_2^+/D^+ ion signal ratio are observed between vibrational and rotational levels as shown in Fig. 2; this phenomenon is also observed in the other isotopes.

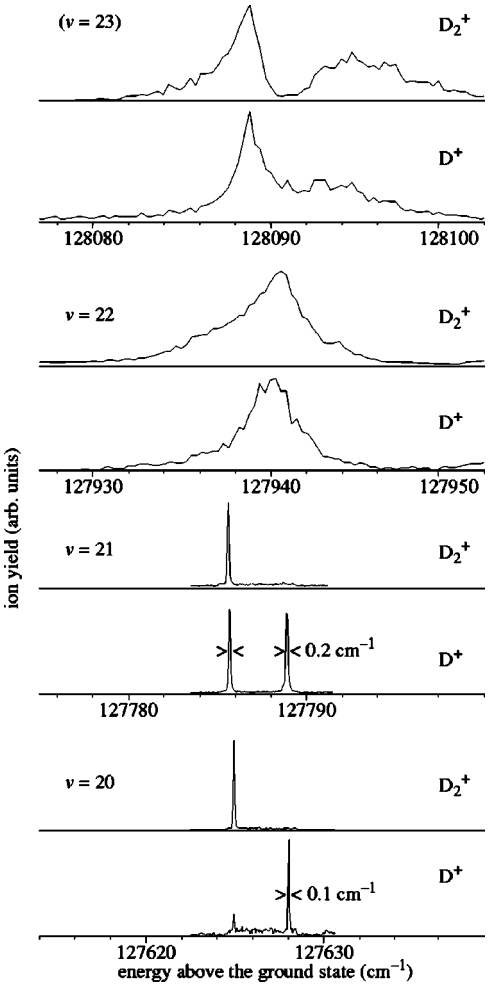

FIG. 2. Sequence of $\bar{H}$ rovibronic levels in D_2 with $v=20-22$, $J=0$ and 2, excited from the B, $v=27$, $J=1$ intermediate state; D_2^+ and D^+ signals monitor autoionization and predissociation, respectively. A complex resonance is observed at the energy where the $v=23$ level is predicted.

Lifetimes τ of broadened resonances are deduced from observed widths $\Delta\nu$ after deconvolution with the laser width: $\tau=1/(2\pi c\Delta\nu)$ ($\Delta\nu$ in cm^{-1}). In cases of complex resonances the total width is taken. Obviously such a structure does not correspond to a single exponential in the time domain, and the lifetime thus derived for the $\bar{H}$ state corresponds roughly to the fastest time scale related to the decay of the resonance. Lifetimes thus derived are listed in Table I. For some levels spectra were taken with different intermediate states, showing linewidth variations in the order of only 10%–20%; we assume an uncertainty of 20% as a conservative value. The uncertainty is larger for lines that are only slightly broader than the laser linewidth of ≈ 0.07 cm^{-1}; only lines broader than 0.1 cm^{-1} are considered.

For all but the highest vibrational $\bar{H}$ levels narrow lines are observed, including levels above the ionization limit. Lifetime measurements in the time domain are performed for rovibrational levels with $J=0-3$ and $v=6-12$ in H_2 and $v=15-19$ in D_2. Figure 3 shows two recordings of the $\bar{H}$, $v=8$, $J=3$, taken with two wavelengths of the delayed pulse. A striking difference appears in the respective measured decay times: 114 ns for an ionization pulse at 355 nm and 33 ns at 433 nm. Comparable differences between measurements with these two wavelengths are found for all low vibrational levels that were investigated. As will be discussed in the following section, additional ionization effects occur with a pulse at 355 nm; only the measurement at 433 nm reflects the actual lifetime of the $\bar{H}$ quantum levels.

TABLE I. Experimental lifetimes (in ps) of rovibrational $\bar{H}$ levels in H_2, D_2, and HD and $\bar{B}$ levels in HD, deduced from observed linewidths; estimated relative uncertainty 20%. Calculated tunneling times are given in the last column.

	$J=0$	$J=1$	$J=2$	$J=3$	$J=4$	$J=5$	Calc.
			H_2				
$v=14$	21	40	34	27	48	21	14
$v=15$	7.9	3.7	5.5	5.6			1.4
			D_2				
$v=21$	61	>100	47	28	27		20
$v=22$	1.0	6.8	2.8	7.0	24	7.7	2.6
$v=23$[a]	0.54[b]		0.54[b]				
			HD: $\bar{H}$ state				
$v=16$	36	34	22	32			63
$v=17$	4.4	2.7	8.5	11			6.7
$v=18$	20	8.2	5.2	1.0			0.9
$v=19$[a]	0.9	7.9	0.6	1.9			
			HD : $\bar{B}$ state				
$v=16$	45	47	61	36			
$v=17$	20	12	24	52			
$v=18$	40	30	24	16			
$v=19$	5.8	5.9	4.3	1.5			
$v=20$	4[c]	2.4	3.4	2.5			
$v=21$	2.1[b]	1.5[b]	2.1[b]	1.5[b]			
$v=22$	0.3[b]	0.3[b]	0.3[b]	0.3[b]			

[a]Resonance above adiabatic potential barrier.
[b]Based on total width of a resonance with complicated shape; rotational assignment uncertain, possibly overlapping $J=0$ and 2, or $J=1$ and 3; uncertainty 50%.
[c]Uncertainty 50%.

Experimentally determined lifetimes in H_2 and D_2 are shown in Table II; in HD no lifetimes longer than 5 ns are found. The uncertainty is estimated from the scatter in the results of repeated measurements performed for some of the states. Lifetimes of the highest two vibrational levels in each isotopomer are significantly shortened. For lower levels

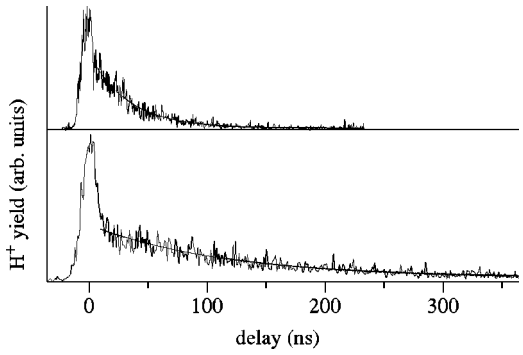

FIG. 3. Time domain measurement of $\bar{H}$, $v=8$, $J=3$ in H_2, showing an exponential in the H^+ signal with $\tau=33$ ns (ionizing pulse at 433 nm, upper trace); the hump at $t=0$ occurs due to laser pulses overlapping in time. With an ionizing pulse at 355 nm (lower trace) the signal decreases more slowly due to delayed ionization of metastable $H(2s)$ fragments (see text).

TABLE II. Observed lifetimes (in ns) of rovibrational $\bar{H}$ states in H_2 and D_2 measured in the time domain. Estimated relative uncertainty 10%. Calculated tunneling times are given if shorter than 1 μs.

	$J=0$	$J=1$	$J=2$	$J=3$	Calc.
			H_2		
$v=6$		28		30	
$v=7$		19		27	
$v=8$	22	19	28	32	
$v=9$	28	32	30	42	
$v=10$	41	29	33	27	190
$v=11$	23	18	14	16	16
$v=12$	22	8	13	10	1.3
			D_2		
$v=15$	56	58	58	55	
$v=16$	56	48	50	56	
$v=17$	46	50	51	57	220
$v=18$	35	10		28	15
$v=19$	10	16	23	<5	1.5

some nonsystematic variation with v and J occurs; typical values are 30 ns in H_2 and 60 ns in D_2. These lifetimes are considerably shorter than the predicted radiative lifetime of about 140 ns, which was calculated for fluorescence in the $\bar{H}\,^1\Sigma_g^+ - B\,^1\Sigma_u^+$ system, the only system of bound–bound transitions.[19] This deviation and the significant difference of lifetimes in D_2 and H_2 strongly suggest that other decay processes are dominant.

B. Identification of decay processes

For identification of the decay channels from experimental spectra it is important to consider all processes that may give rise to ion signal. Possible decay channels of excited $\bar{H}$ rovibrational states are indicated in Fig. 4 together with additional ionization pathways induced by the third laser pulse. The $\bar{H}$ outer well state may decay by fluorescence, by predissociation due to interaction with the $H(n=1)+H(n=2)$ continuum, and by tunneling of the nuclear motion through the $H\bar{H}$ potential barrier towards short internuclear separation R. After tunneling further decay at small R may occur by autoionization when energetically possible, by fluorescence, or by predissociation. The two predissociation processes may be called direct and indirect predissociation, respectively.

H_2^+ ions are produced by exciting an $\bar{H}$ level above the ionization limit with 1 XUV+1 visible photon, leading to autoionization. Tunneling through the barrier must be involved because only the lowest vibrational levels of the $X\,^2\Sigma_g^+$ ground state of the H_2^+ ion at small internuclear distance are energetically available. The $\bar{H}$, $v=10$ level in H_2 is the lowest one for which autoionization is observed, although it is energetically possible for $v \geqslant 5$. All higher levels that show strong autoionization have a short lifetime. As long as the intensity of the second laser is kept sufficiently low, the H_2^+ ion signal is specific for autoionization; linear dependence of the ion signal as a function of laser pulse energy shows that no additional photon is involved. At high intensities of the second laser pulse, however, as applied for some transitions with small Franck–Condon factor to increase the population of the $\bar{H}$ state, a nonlinear dependence of the H_2^+ yield on pulse energy is observed, suggesting that multi-photon ionization effects are responsible.

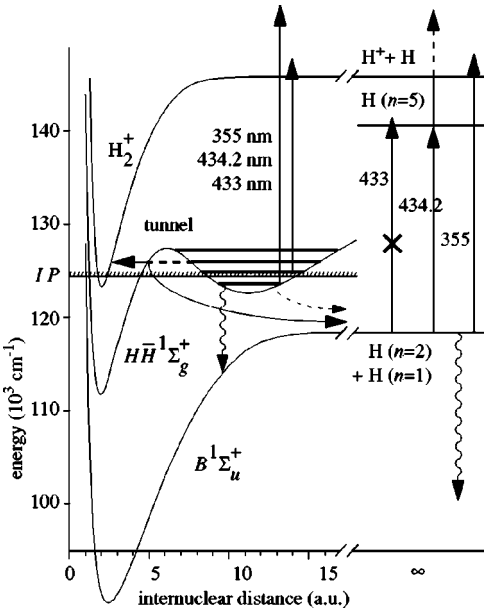

FIG. 4. Dynamical behavior of the $\bar{H}$ state: Fluorescence, tunneling through the $H\bar{H}$ potential barrier, autoionization at small internuclear distance, and predissociation into the $H(n=2)+H(n=1)$ continua. Upward vertical arrows denote optical excitation of the $\bar{H}$ state of its decay products. $H(n=2)$ fragments can be ionized by the third pulse, either by one photon at 355 nm or through two-photon ionization with resonance enhancement on the $H(n=2)\rightarrow(n=5)$ transition.

For H^+ production three pathways are feasible (cf. Fig. 4): Dissociative ionization of an excited neutral H_2 molecule, photodissociation of H_2^+ originating from autoionization, and photoionization of neutral hydrogen atoms originating from predissociation. All processes require a third laser pulse and can, therefore, be distinguished by the effect of using different wavelengths and the ion signal dependence on pulse delay.

The first pathway is the generic process for the detection of $\bar{H}$ states as described above; all wavelengths used for the ionization pulse provide sufficient photon energy. A signature of this process is an exponential signal decrease as a function of pulse delay, determined by the lifetime of the excited molecular state. The second pathway cannot play a significant role in the observed spectra, although it is energetically allowed: Photodissociation of H_2^+ must involve an electronic transition to the repulsive excited $a\,^2\Sigma_u^+$ state, but the energy of a 355 nm photon is not sufficient for the low-lying ro-vibrational ground state levels of H_2^+ produced in the investigated energy range. Accordingly, most of the resonances with a high H_2^+ yield go along with a negligible H^+ signal. The third pathway includes ionization of hydrogen atoms in the $2s$ and $2p$ states. Both can be ionized by a single photon at 355 nm or two photons at 434.2 nm resonant with the B_γ transition. The $2p$ state has a lifetime of only 1.6 ns and, therefore, decays predominantly via Lyman-α fluorescence unless the ionization pulse is temporally overlapped with the excitation pulses. The $2s$ state is metastable, giving

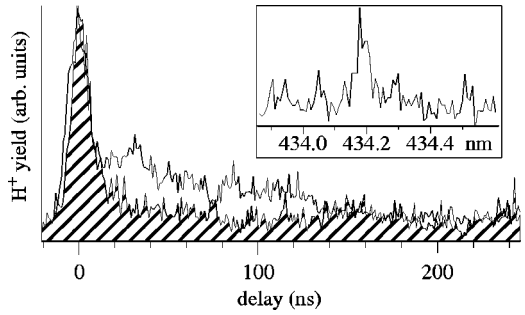

FIG. 5. H^+ signal from $\bar{H}$, $v=14$, $J=2$ in H_2 as a function of the ionization pulse delay. H^+ signal is observed only when the ionizing pulse is resonant with the atomic $H(n=2)\rightarrow(n=5)$ transition (434.2 nm, upper trace), but not at 433 nm (lower trace). The inset shows a wavelength scan of the ionization pulse with a constant delay of 100 ns.

rise to an essentially delay independent H^+ signal.

All low vibrational $\bar{H}$ levels are observed in the H^+ signal, irrespective of the wavelength used for the ionization pulse; no H_2^+ is observed in all these cases. However, differences in decay times obtained in lifetime measurements of these states with ionization radiation at 355 and 433 nm (cf. Fig. 3) suggest that hydrogen atoms in the metastable $2s$ state are detected by the delayed 355 nm pulse. Fly-out of these fast dissociation fragments from the interaction volume of $\approx 5\times 5\times 5$ mm^3 may give the false impression of a decay process. 433 nm photons can only produce ions via dissociative ionization of the excited molecule, providing a reliable lifetime measurement of the $\bar{H}$ state.

The detection of $H(2s)$ atoms for all low vibrational states means that they decay partly by a dissociative process, which may be related to the unexpected lifetime difference between H_2 and D_2. Direct predissociation of the $\bar{H}$ state into dissociative continua of lower-lying electronic states is a possibility; although calculated predissociation rates due to nonadiabatic coupling with the EF state at large R are too small by orders of magnitude to account for the observed lifetimes (10^{-6} s^{-1} for $\bar{H}$, $v=0$,[19]) coupling with other continua at the $n=2$ dissociation limit may contribute. Selection rules allow for predissociation by the $GK\,^1\Sigma_g^+$ and $I\,^1\Pi_g$ states. The possibility of indirect predissociation after tunneling through the $H\bar{H}$ potential barrier will be discussed below.

An additional decay process leading to $H(n=2)$ decay products is radiative dissociation. Next to decay in the $\bar{H}-B$ system dipole selection rules allow for decay to the $B'\,^1\Sigma_u^+$ and $C\,^1\Pi_u$ states; their potentials have almost reached the $H(n=1)+H(n=2)$ asymptote at the internuclear distance of the $\bar{H}$ state, favoring radiative dissociation over bound transitions in these systems. These decay channels may contribute to shortening of the lifetime by an unknown amount, but no isotope dependence is expected as a result of radiative processes.

For several higher vibrational levels H^+ ions are observed with a delayed ionization pulse at 355 nm; this signal is also obtained with $\lambda=434.2$ nm (B_γ), while it is absent for $\lambda=433$ nm, as shown for the $v=14$, $J=2$ state in H_2 in Fig. 5. The inset shows the atomic $(n=2)\rightarrow(n=5)$ resonance in the H^+ signal as the ionization laser is tuned in wavelength at a constant delay of 100 ns, identifying atoms in the metastable $2s$ state as the major source of the H^+ signal. The nonexponential decrease of the signal with time is clearly an artefact due to fly-out and has no relation with lifetimes. Other (nonautoionizing) high vibrational states give rise to a strong H^+ signal that appears only when the ionization pulse is temporally overlapped with the other laser pulses. These levels are broadened, therefore, their lifetime is short enough to prevent dissociative ionization of the excited state itself; for the same reason no H^+ at all is observed for autoionizing states with comparable lifetimes. Thus fast dissociation leading to $H(2p)$ atoms, which are ionized by the third laser pulse, is identified as decay process.

C. Tunneling towards small internuclear distance

Autoionization and what was called indirect predissociation both require tunneling through the $H\bar{H}$ potential barrier towards short internuclear distance. The strength of this coupling can be quantified: Semiclassical tunneling rates are given by[17]

$$\Gamma_v = f_v p(E_v), \tag{2}$$

with f_v the classical vibration frequency of the $\bar{H}$ level and $p(E_v)$ the permeability of the potential barrier at a given level energy E_v; the permeability is given in JWKB (Jeffreys–Wentzel–Kramers–Brillouin) approximation by

$$p(E)=\exp\left(-2\int\left\{\frac{2\mu}{\hbar^2}[V(R)-E]\right\}^{1/2}dR\right). \tag{3}$$

μ is the reduced mass of nuclear motion and $V(R)$ is the adiabatic potential, given by the Born-Oppenheimer potential with (isotope-dependent) adiabatic shifts added.[18] The integration is taken over the classically forbidden region $[V(R)>E]$; vibration frequencies f_v are approximated by the vibrational spacing, taking for each level the mean of the spacings to the adjacent higher and lower level.

Tunneling rates calculated with this model are shown in Fig. 6; values for the lowest and highest observed vibrational levels in the isotopes H_2, HD, and D_2 differ by up to 18 orders of magnitude and increase roughly by a factor of 10 per vibrational level. These rates form an upper bound to the decay rates involving tunneling; when decay rates of states reached at small internuclear distance are smaller than the tunneling rate, the decay of $\bar{H}$ states may be slower than calculated, but tunneling remains the limiting factor in case of very fast further decay.

Two regions of different dynamical behavior can be discerned. Tunneling rates of vibrational states in region I, part of which even lie up to 2000 cm^{-1} above the ionization threshold, are smaller than the predicted fluorescence rate of 7×10^6 s^{-1}.[19] In region II tunneling rates are large enough to allow for autoionization and indirect predissociation at small internuclear distance to become dominant. Tunneling rates below the shaded interval result in lifetimes ($\tau>5$ ns) that exceed the laser pulse duration and are, therefore, accessible

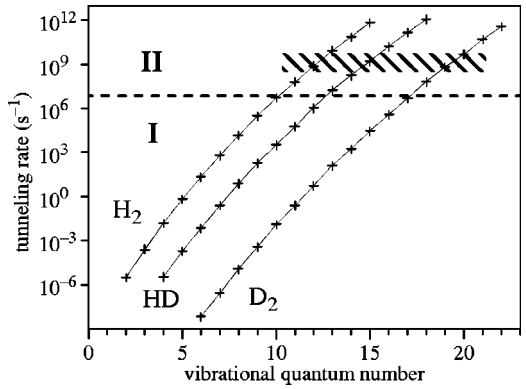

FIG. 6. Tunneling rates of $\bar{H}$ vibrational levels in H_2, HD, and D_2 through the potential barrier in the JWKB approximation [Eq. (3)], based on the Born–Oppenheimer potential and adiabatic corrections for the isotopes from Ref. 18. The dashed line separates region I of dominant fluorescence from region II, where decay after tunneling dominates. Lifetimes of states below the shaded region exceed are studied in the time domain, whereas lifetimes above that interval show up as line broadening.

for investigation in the time domain, whereas decay rates lying above that interval (corresponding to $\tau<100$ ps) are studied in the frequency domain, showing up as line broadening exceeding laser linewidth.

In Tables I and II observed lifetimes are compared with the times corresponding to the calculated tunneling rates. Higher vibrational levels, for which decay via tunneling dominates, have lifetimes that are in general longer than calculated within one order of magnitude. This indicates that decay rates of high vibrational $\bar{H}$ levels are indeed limited by tunneling rates through the potential barrier, but also influenced by the subsequent decay dynamics. The most extreme example of the latter is the $v=18$, $J=0$ state in HD the lifetime of which is 20 times the calculated tunneling time. Considerable variation with J quantum number is found (e.g., a factor of 26 between $v=22$, $J=0$ and 4 in D_2), while calculated rates do not differ significantly.

D. Additional effects in HD

In HD the situation is more complicated because of breaking of the $g-u$ symmetry, leading to strong interaction between the $\bar{H}\,^1\Sigma_g^+$ and $\bar{B}\,^1\Sigma_u^+$ states.[14,15] Equation (2) cannot be applied strictly because there is no well-defined semiclassical vibrational frequency for individual states, which have all mixed $\bar{H}$ and $\bar{B}$ character. However, an approximate result for the semiclassical tunneling rates is obtained for levels with predominant $\bar{H}$ character by treating them as if they were pure; the results are included in Fig. 6. Experimental lifetimes deduced from observed linewidths are included in Table I. Time-domain measurements turn out to be impossible because lifetimes of all observed low vibrational levels are shorter than the laser pulses. This may be explained by dominant radiative decay to the ground state, not dipole forbidden in HD, in contrast to H_2 and D_2. The $\bar{B}$ state corresponds to the outer well of the double-well potential $B''\bar{B}\,^1\Sigma_u^+$,[14,20] similar in shape to the $\bar{H}$ state, except for the barrier at intermediate internuclear distance being ≈ 3400 cm^{-1} higher than in the $H\bar{H}\,^1\Sigma_g^+$ potential. Treating the $\bar{B}$ state in the same way as the $\bar{H}$ state [Eq. (3)] leads to values for the barrier permeability in the $B''\bar{B}$ potential orders of magnitude smaller than for $H\bar{H}$. The tunneling rate for the highest observed level of dominant $\bar{B}$ character ($v=22$) is only 2×10^5 s^{-1}, which means that $\bar{B}$ levels should be narrow if there was no interaction with the $\bar{H}$ state.

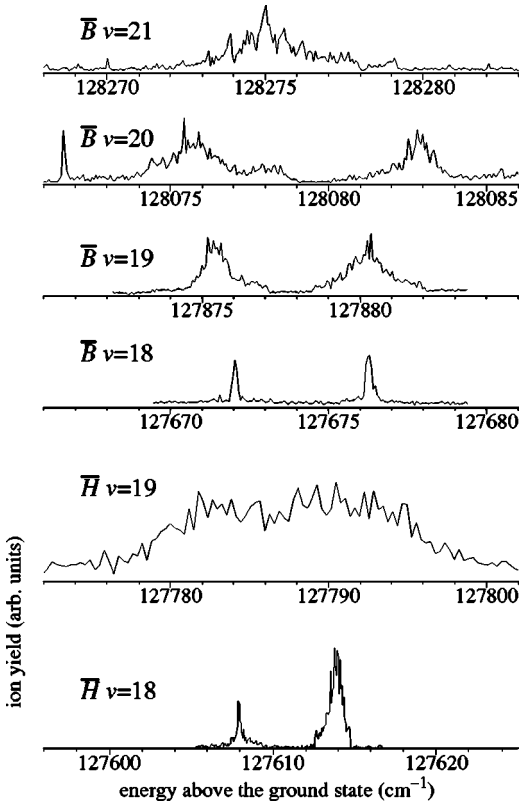

FIG. 7. Sequence of $\bar{H}$ and $\bar{B}$ vibrational levels in HD close to the top of the $H\bar{H}$ potential barrier. Levels of dominant $\bar{H}$ character quickly broaden and disappear in the continuum with increasing energy. $\bar{B}$ levels remain bound, but are broadened by $g-u$ breaking interaction with the short-lived $H\bar{H}$ state; tunneling through the $B''\bar{B}$ barrier is not involved.

However, levels with $v\geqslant 16$ show line broadening beyond the laser linewidth; in Fig. 7 we show spectra of levels formally assigned as $\bar{B}$ with $v=18$–21, $J=0$ and 2, which lie far below the $B''\bar{B}$ potential barrier, but in the energy region close to the barrier in the $H\bar{H}$ potential, to which they are coupled. Starting from $\bar{B}$, $v=19$ (the first one higher in energy than the barrier of $H\bar{H}$) levels are broad and the rotational structure is gradually washed out; in contrast to the $\bar{H}$ levels in HD as well as in H_2 and D_2 (cf. Fig. 2), these $\bar{B}$ levels do not completely disappear in the continuum. Autoionization shows a strong enhancement close to the expected rovibrational line positions, however, with a complicated structure superimposed. Corresponding lifetimes are given in Table I, where the widths of the highest levels are again taken as the widths of the complete resonance structures. This lifetime reduction of the $\bar{B}$ state indicates that efficient decay occurs through the $H\bar{H}$ admixture due to $g-u$ sym-

metry breaking in HD; the $H\bar{H}$ component is not confined to large internuclear distance in this energy range, in contrast to the dominant $\bar{B}$ component.

IV. CONCLUSION

In the present paper we report on an experimental study of the decay dynamics of excited states in the hydrogen molecule, confined at large internuclear distance in the energy region above the ionization threshold and the $(n=2)$ dissociation limit. The decay dynamics of the $\bar{H}\,^1\Sigma_g^+$ state strongly depends on the vibrational excitation and shows different features in homonuclear and heteronuclear isotopomers, in the latter case involving the $\bar{B}\,^1\Sigma_u^+$ state. Global patterns of the lifetimes of vibrational states are explained in a semiclassical model.

High vibrational $\bar{H}$ levels in all isotopomers ($v \geqslant 12$ in H_2, $v \geqslant 15$ in HD, $v \geqslant 20$ and D_2) mainly decay by autoionization or predissociation; the highest levels are substantially broadened, indicating very short lifetimes. These observations are explained with fair quantitative agreement by tunneling through the $H\bar{H}$ potential barrier towards small internuclear distance R and subsequent fast decay, resulting in a competition between dissociation and autoionization. Above the barrier no individual resonances belonging to adiabatic vibrational $H\bar{H}$ levels can be distinguished. Nonadiabatic couplings at short internuclear distance R are known to be strong, as they give rise to broad resonances[6] and shifts in bound levels of up to 100 cm^{-1}.[21,22] They originate from interaction between electronic states that correlate with the $(n=2)+(n=1)$ dissociation continua with higher electronic states.

Lower rovibrational $\bar{H}$ states in H_2 $(v=6-10)$ and D_2 $(v=15-17)$ are found to be long-lived. Autoionization of these levels, lying well beyond the ionization limit, is dynamically inhibited by the potential barrier. Lifetimes are measured through dissociative ionization of the bound molecular state induced by a laser pulse with variable delay and turn out to be considerably shorter than the predicted 140 ns,[19] which was based on fluorescence in bound–bound transitions, neglecting radiative dissociation. A significant isotope dependence of a factor of 2 is found for H_2 and D_2, which cannot be explained by radiative processes. The additional detection of metastable H$(2s)$ fragments suggests that predissociation occurs, although indirect predissociation after tunneling through the $H\bar{H}$ potential barrier can be excluded: Tunneling probabilities are too small by orders of magnitude and decrease steeply with lower vibrational excitation. While direct predissociation into the continuum of the $EF\,^1\Sigma_g^+$ state is probably too weak, dissociation into the $GK\,^1\Sigma_g^+$ and $I\,^1\Pi_g$ states may be the lifetime limiting effect.

In HD all observed $\bar{H}$ levels are short-lived. Lifetimes of low v levels are shortened due to radiative decay to the ground state, which is not only an allowed transition in HD, but it is expected to be strong due to major $g-u$ mixing of the $\bar{H}$ and the $\bar{B}$ state;[15] the $\bar{B}$ state quickly decays to the ground state by fluorescence. Lifetimes of all observed $\bar{B}$ levels in HD are short. $\bar{B}$ levels in HD with moderately high v, which should still be strongly confined by a high potential barrier if $g-u$ symmetry was not broken, are strongly broadened by coupling with the $\bar{H}$ state.

Branching ratios between predissociation and autoionization of the $\bar{H}$ state are found to change without an apparent pattern even between rotational states of the same vibrational level and additional structure is observed in broadened lines; a quantitative explanation requires further theoretical research on interactions between bound states and the various continua at small internuclear distance in the $^1\Lambda_g$ manifold of the hydrogen molecule. The same holds for quantifying the effects of direct predissociation and radiative dissociation on the lifetime of low vibrational $\bar{H}$ states. For a treatment of HD the interaction with $^1\Lambda_u$ states has to be included as well. This work may stimulate further theoretical development leading to understanding of the complex intramolecular dynamical behavior in the smallest molecule.

ACKNOWLEDGMENT

The authors acknowledge the Vrije Universiteit for a special (USF)-project grant.

[1] W. A. Chupka and J. Berkowitz, J. Chem. Phys. **51**, 4244 (1969).
[2] P. Borrell and P. M. Guyon, J. Chem. Phys. **66**, 818 (1977).
[3] M. Glass-Maujean, J. Chem. Phys. **85**, 4830 (1986).
[4] S. Arai, T. Kamosaki, M. Ukai, K. Shinsaka, Y. Hatano, Y. Ito, H. Koizumi, A. Yagishita, K. Ito, and K. Tanaka, J. Chem. Phys. **88**, 3016 (1988).
[5] K. Ito, R. I. Hall, and M. Ukai, J. Chem. Phys. **104**, 8449 (1996).
[6] H. Rottke and K. H. Welge, J. Chem. Phys. **97**, 908 (1992).
[7] A. H. Kung, R. H. Page, R. J. Larkin, Y. R. Shen, and Y. T. Lee, Phys. Rev. Lett. **56**, 328 (1986).
[8] S. T. Pratt, P. M. Dehmer, and J. L. Dehmer, J. Chem. Phys. **97**, 3038 (1992).
[9] C. R. Scheper, W. J. Buma, C. A. de Lange, and W. J. van der Zande, J. Chem. Phys. **109**, 8319 (1998).
[10] C. R. Scheper, C. A. de Lange, A. de Lange, E. Reinhold, and W. Ubachs, Chem. Phys. Lett. **312**, 131 (1999).
[11] Ch. Jungen, S. T. Pratt, and S. C. Ross, J. Phys. Chem. **99**, 1700 (1995).
[12] Ch. Jungen and S. C. Ross, Phys. Rev. A **55**, R2503 (1997).
[13] E. Reinhold, W. Hogervorst, and W. Ubachs, Phys. Rev. Lett. **78**, 2543 (1997).
[14] E. Reinhold, W. Hogervorst, W. Ubachs, and L. Wolniewicz, Phys. Rev. A **60**, 1258 (1999).
[15] E. Reinhold, W. Hogervorst, and W. Ubachs, Chem. Phys. Lett. **296**, 411 (1998).
[16] E. Reinhold, A. de Lange, W. Hogervorst, and W. Ubachs, J. Chem. Phys. **109**, 9772 (1998).
[17] P. Senn and K. Dressler, J. Chem. Phys. **87**, 1205 (1987).
[18] L. Wolniewicz, J. Chem. Phys. **108**, 1499 (1998).
[19] L. Wolniewicz and K. Dressler, J. Mol. Spectrosc. **77**, 286 (1979).
[20] W. Kołos, J. Mol. Spectrosc. **62**, 429 (1976).
[21] P. Quadrelli, K. Dressler, and L. Wolniewicz, J. Chem. Phys. **92**, 7461 (1990).
[22] S. Yu and K. Dressler, J. Chem. Phys. **101**, 7692 (1994).